Journal of
MATERIALS RESEARCH

Nucleation mechanisms in chemically vapor-deposited mullite coatings on SiC

Ping Hou, S.N. Basu,[a] and V.K. Sarin
Department of Manufacturing Engineering, Boston University, 15 St. Mary's Street, Boston, Massachusetts 02215

(Received 7 December 1998; accepted 19 April 1999)

Dense, uniform, and adherent chemically vapor-deposited mullite coatings were deposited on SiC substrates using the $AlCl_3$–$SiCl_4$–H_2–CO_2 system. Typical coating morphology consisted of a thin interfacial layer of γ–Al_2O_3 nanocrystallites embedded within a vitreous SiO_2-based matrix. When a critical Al/Si ratio of 3.2 ± 0.29 was reached within this nanocrystalline layer, mullite crystals nucleated and grew as columnar grains. The thickness of the nanocrystalline layer decreased as the input $AlCl_3/SiCl_4$ ratio was increased. In all cases, the Al/Si composition in the coating increased from the coating/substrate interface to the coating surface. Critical factors leading to the nucleation and growth of mullite crystals are discussed in this article.

I. INTRODUCTION

Silicon-based ceramics (Si_3N_4 and SiC) are currently the leading candidate materials for high-temperature applications because of their excellent mechanical properties, such as high-temperature strength and low-creep rate. However, their susceptibility to high-temperature corrosion and contact-stress damage has led to extensive research to develop protective coatings for these ceramics. Mullite ($3Al_2O_3 \cdot 2SiO_2$), due to its thermal stability, superior corrosion resistance at high temperatures and its thermal expansion match with SiC, has been targeted as a prime candidate coating material.

Traditionally, mullite has been produced by mixing precursors containing Al and Si and heating to temperatures higher than 1000 °C.[1] The technique of producing mullite coatings by chemical vapor deposition (CVD) has only recently been developed.[2,3] Using this technique, dense, uniform mullite coatings can be directly deposited on substrates of complex shapes at a relatively low temperature of around 950 °C. These mullite coatings show promise as protective barriers for Si-based ceramics in the corrosive high-temperature environments.

Formation of bulk mullite is a complex process that strongly depends on the synthesis methods used and the nature of starting materials. These factors determine the mullitization temperature, compositional homogeneity of the mullite formed, and the distribution of point defects in mullite. This article examines the microstructures of CVD mullite coatings grown under conditions of varying input $AlCl_3/SiCl_4$ gas ratio. The results are discussed in light of critical microstructural features needed for the nucleation of mullite.

II. EXPERIMENTAL DETAILS

Mullite coatings were deposited by chemical vapor deposition using the $AlCl_3$–$SiCl_4$–H_2–CO_2 system on 3 × 4 × 20 mm^3 Hexoloy® SiC substrates from Carborundum. The bars, polished to a 600-grit surface finish, were first ultrasonically cleaned in acetone, then alcohol and finally heated (within the deposition chamber) in H_2 at 75 torr at 950 °C for 10 min for high-temperature surface cleaning. Deposition of the mullite coating by CVD was then carried out by the overall reaction:

$$6\,AlCl_3 + 2\,SiCl_4 + 13\,CO_2 + 13\,H_2 = 3\,Al_2O_3 \cdot 2\,SiO_2 + 13\,CO + 26\,HCl.$$

The temperature and total pressure in the reaction chamber were fixed at 950 °C and 75 torr. The stoichiometry of the input $AlCl_3/SiCl_4$ ratio was changed from 1 to 4 by adjusting their flow rates and keeping the total metal chloride flow ($AlCl_3$ and $SiCl_4$) constant. All reactant gases were mixed just before introduction into the hot-wall reactor. Unless otherwise stated, the total coating deposition time was 2 h.

The coatings were examined by x-ray diffraction (XRD) for phase identification, using monochromatic Cu K_α radiation and a 0.02° step size with a 2.0-s dwell time. The surface and cross-section morphologies of the coatings were examined by a JEOL6100 scanning electron microscope (SEM), while electron transparent cross sections were examined in a JEOL 2010FX transmission

[a]Address all correspondence to this author.
e-mail: basu@bu.edu

electron microscope (TEM). The chemical composition of the coatings were analyzed using a VG-HB603 scanning-transmission electron microscopy (STEM), using a 4-nm electron beam.

III. RESULTS AND DISCUSSION

Typical SEM micrographs of the surface and fracture cross section of a CVD-mullite coating (grown using an $AlCl_3/SiCl_4$ input ratio of 2) is shown in Fig. 1. The coatings were found to be dense, uniform, and adherent. The XRD spectrum of the coating (Fig. 2) confirmed that the CVD coatings were mullite. One interesting observation was that the structure of mullite appeared to be tetragonal, as evidenced by the lack of splitting of the (120)/(210), (021/201), and (230)/(320) peaks. The equilibrium structure of mullite is orthorhombic, with lattice parameters of $a = 0.7546$, $b = 0.7690$, and $c = 0.288$ nm.[4]

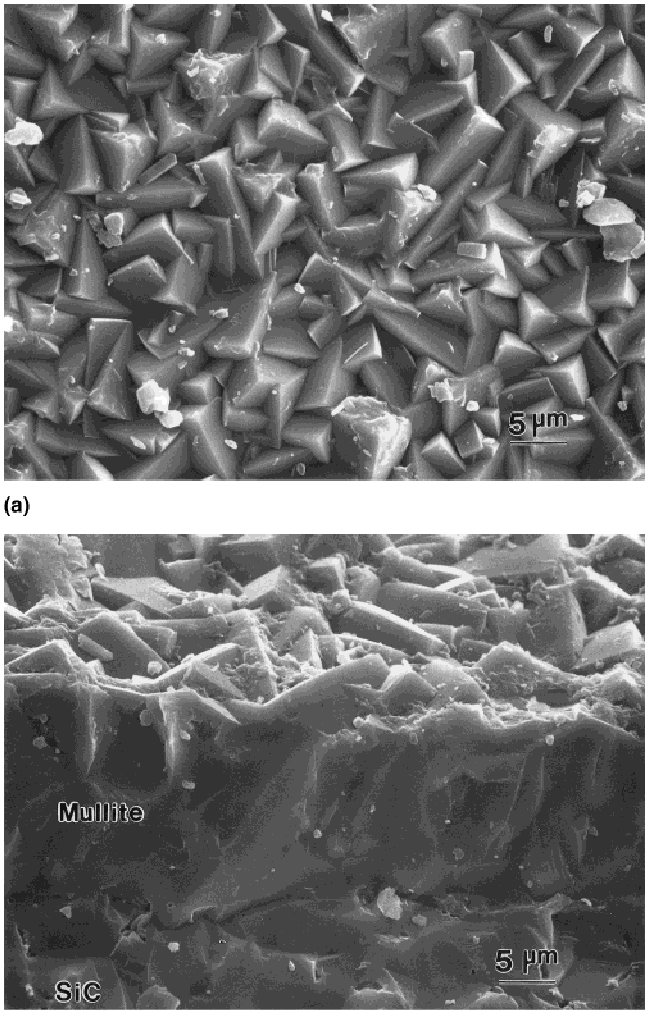

FIG. 1. SEM micrographs of (a) the surface and (b) a cross section of a mullite coating on SiC.

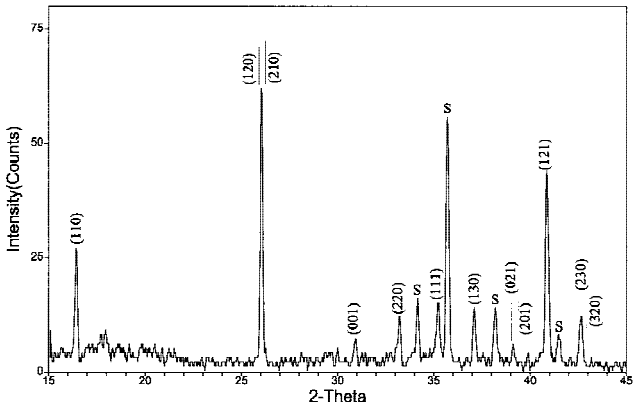

FIG. 2. XRD spectrum of a mullite coating on SiC.

Figure 3(a) shows a cross-section TEM bright-field micrograph of the coating. Two distinct layers can be seen within the coating. The top layer consists of columnar grains, above what appears to be a noncrystalline interfacial layer. However, the selected area diffraction (SAD) pattern from this region contained a set of concentric rings [Fig. 3(b)], indicating the presence of fine γ–Al_2O_3 crystallites with no preferred orientation. A high-resolution analysis of this region [Fig. 3(c)] indicated these γ–Al_2O_3 crystallites to be of the order of several nanometers in size (one such crystallite is outlined in the figure), and embedded within a vitreous matrix. From hereon, we shall refer to this layer as the nanocrystalline layer. Compositional analysis of this region in a STEM showed the presence of both Al and Si in this layer, implying that the vitreous matrix is the Si-containing phase. The close spacing of the nanocrystallites made it impossible to get an EDX spectrum from the vitreous matrix alone, without interference from surrounding γ–Al_2O_3 nanocrystallites.

To ascertain the identity of the vitreous matrix, a coating with only the nanocrystalline layer was grown. No diffraction peaks from either the vitreous matrix or the γ–Al_2O_3 phase were observed [Fig. 4(a)], which is consistent with its very fine crystallite size. However, after the film was annealed at 1200 °C for 100 h the XRD spectrum showed the presence of the major (101) diffraction peak of cristobalite [Fig. 4(b)], which was shifted very slightly to the left ($\Delta 2\theta = 0.21°$) as compared to its listed standard position in the Powder Diffraction File.[4] This corresponds to a slight dilation of the cristobalite lattice. There can be two interpretations of this result. The first explanation is that the vitreous matrix crystallized into pure cristobalite with a residual tensile stress, because cristobalite has a higher density ($\rho = 2.33$ gm/cm^3) than the vitreous silica matrix ($\rho = 2.21$ gm/cm^3) it replaced, while the γ–Al_2O_3 crystallites did not coarsen sufficiently to become detectable by XRD. The second explanation is that interdiffusion oc-

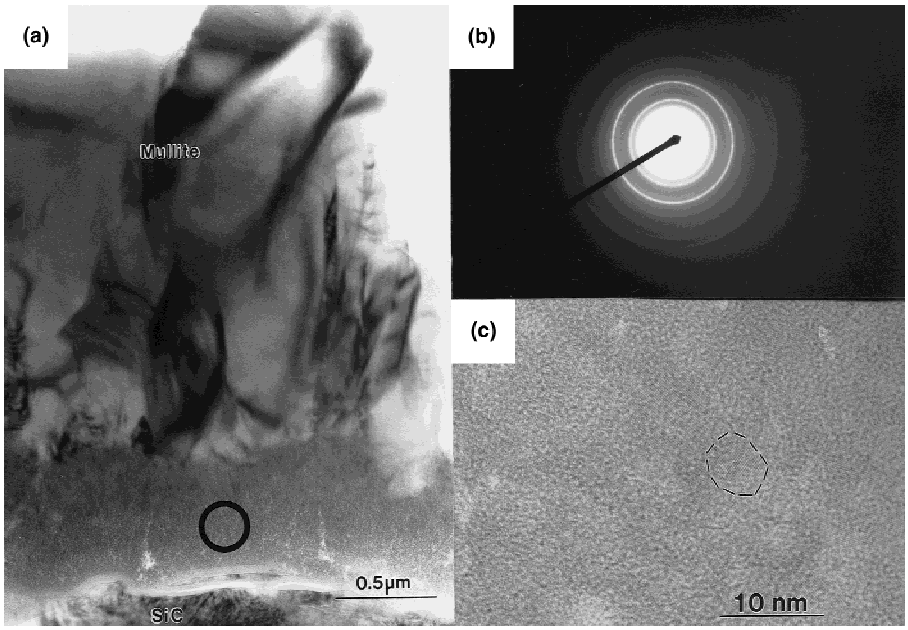

FIG. 3. (a) TEM bright-field cross-sectional micrograph of CVD mullite coating on SiC. (b) SAD pattern from nanocrystalline layer. (c) High-resolution micrograph of nanocrystalline layer, showing γ–Al_2O_3 nanocrystallites, one of which is marked by the dotted line.

curred between the vitreous matrix and the γ–Al_2O_3 crystallites during the anneal, with the interdiffused phase crystallizing into a cristobalite structure, whose lattice parameter is dilated as compared to pure cristobalite due to the incorporation of the larger aluminum atoms within the SiO_2 lattice. Such a dilation of the cristobalite lattice due to the formation of a $xSiO_2 \cdot (1-x)Al_2O_3$ phase has been reported in the literature.[4] We believe the latter explanation to be more likely. In either case, the matrix phase is predominantly vitreous silica. Nanocrystallites of γ–Al_2O_3 are embedded within this matrix with interdiffusion probably occurring between the two phases.

Figure 5 shows typical SAD patterns along the major zone axes from the mullite crystals present in the crystalline layer of the coating [upper layer in Fig. 3(a)]. Careful analysis of the [001] diffraction pattern indicates that $a \approx b$, confirming that the unit cell of the deposited mullite crystals is tetragonal. This is in agreement with the XRD data, as discussed previously. The [010] diffraction pattern in Fig. 5 shows a pair of superlattice spots around the {1 0 ½} position. These superlattice spots have been attributed to the presence of domains separated by anti-phase boundaries (APB) within the mullite grains.[5,6] The absence of the {1 0 ½} spot itself, confirms that the structure is mullite and not sillimanite, the latter having a unit cell very similar to mullite, but with a *c*-lattice parameter ($c = 0.5773$ nm) which is double that of mullite.

The above-described microstructure of a nanocrystalline layer at the coating-substrate interface, with a layer of crystalline-mullite grains over the nanocrystalline layer was typical for all coatings grown with different input $AlCl_3/SiCl_4$ ratios. However, we observed that an increase in the $AlCl_3/SiCl_4$ input ratio led to a decrease in the thickness of the nanocrystalline layer. The average nanocrystalline layer thickness was measured for all coatings from cross-sectional TEM micrographs. Figure 6 shows the variation of the nanocrystalline layer thickness with the input $AlCl_3/SiCl_4$ ratio, which is approximately linear.

The composition variation across the coatings was measured on cross-sectional TEM samples in a STEM. In all cases, there was an increase in the Al/Si ratio going from the coating/substrate interface to the coating surface. Figure 7 shows the variation in the Al/Si ratio in the coating grown with an input $AlCl_3/SiCl_4$ ratio of 2. The Al/Si ratio is very low near the nanocrystalline layer/substrate interface, which may be due to the presence of a native silica layer present on the SiC-substrate surface. The Al/Si ratio continues to increase with distance from the coating/substrate interface and reaches a maximum value of 6.39 at the coating surface. This is more than double the Al/Si ratio of 3 in stoichiometric mullite. Cameron studied the formation of Al_2O_3 rich mullite, and explained the incorporation of excess Al atoms as a substitution for Si atoms in the mullite structure by the reaction:[7]

$$2\ Si^{4+} + O^{2-} = 2\ Al^{3+} + O_v$$

where O_v is an oxygen vacancy. Thus, increasing the Al/Si ratio in mullite increases the concentration of oxygen vacancies in the mullite structure. In fact, the chemical formula of mullite can be written as

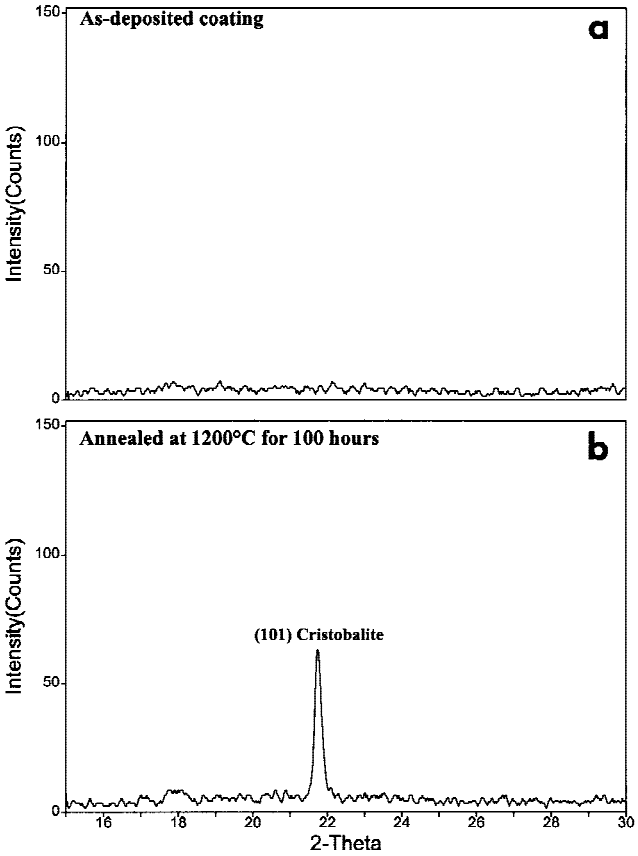

FIG. 4. XRD pattern from nanocrystalline coating in (a) as-deposited state, and (b) after a 100-h anneal at 1200 °C.

$$Al_2{}^{VI}[Al_{2+2x}Si_{2-2x}]^{IV}O_{10-x}$$

where x corresponds to the number of oxygen atoms missing per unit cell. The superscripts, VI and IV correspond to the oxygen coordination of the Al and Si atoms in mullite and will be discussed later in the text.

The pertinent question to ask is what causes the nucleation of the mullite grains from the nanocrystalline layer. To answer this question, the composition of the coating in the vicinity of the nanocrystalline/crystalline interface was studied in detail in the STEM using a 4-nm electron beam. Typically, compositions at 10 locations along this interface in both the nanocrystalline and crystalline regions were measured at a distance of approximately 5 nm on either side of the nanocrystalline/crystalline interface for coatings grown using each $AlCl_3/SiCl_4$-input ratio. It was found that the average compositions on either side of this interface were quite close for all coatings studied, and that this transition from nanocrystallite to crystalline morphology occurred at similar compositions for all coatings, regardless of the input $AlCl_3/SiCl_4$ ratio. This "critical" composition (Al/Si ratio) at which crystalline mullite nucleated in the CVD-mullite coatings investigated was found to be 3.20 ± 0.29 using a single-factor analysis of variance.

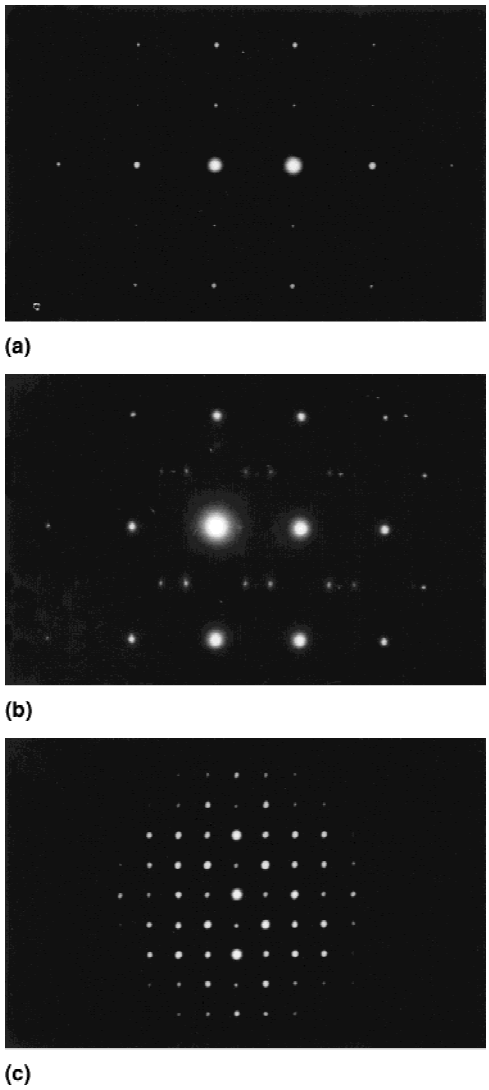

FIG. 5. Selected area (a) [100], (b) [010] and (c) [001] diffraction patterns from columnar mullite grains.

In previous studies, magic-angle spinning nuclear magnetic resonance (MASNMR) spectroscopy has been carried out on mullite grown for sol-gel processes to study the coordination of Al atoms.[8–10] The MASNMR studies showed that both tetrahedrally (AlO_4) and octahedrally (AlO_6) coordinated Al atoms exist when the precursors are mixed at an atomic scale, while only octahedrally coordinated Al atoms exist in physical mixtures of discrete Al_2O_3 and SiO_2 precursors. The number of (AlO_4) also depends on the Al/Si ratio of atomically mixed precursors with the ratio $AlO_4/(AlO_4 + AlO_6)$ reaching the highest value of 0.6 when the Al/Si ratio is 3, corresponding to stoichiometric ($3Al_2O_3 \cdot 2SiO_2$) mullite. This implies that the stoichiometric Al/Si ratio of 3 is the most favorable composition for mullite nucleation in atomically mixed precursors. We conjecture that for the CVD-mullite coatings studied, because the

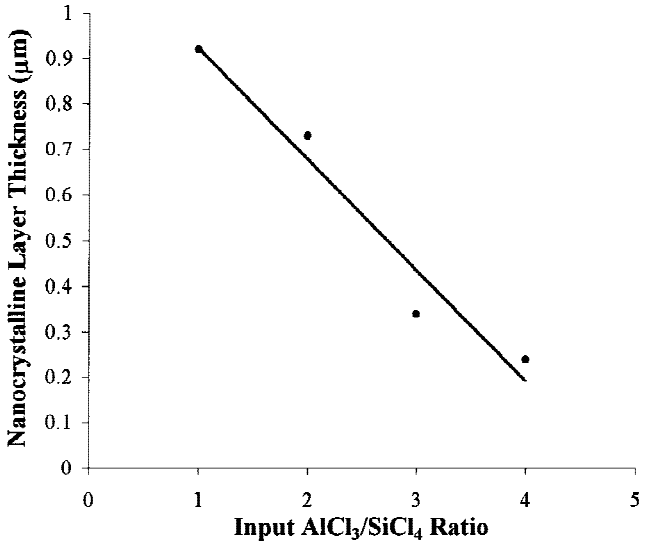

FIG. 6. Plot of nanocrystalline layer thickness as a function of the $AlCl_3/SiCl_4$ input ratio.

Al_2O_3 and SiO_2 precursors within the nanocrystalline layer are mixed at a nanoscale, a slightly higher Al/Si ratio of 3.2 is needed for mullite nucleation, since complete compositional homogenization by interdiffusion between the two phases does not occur under the growth conditions used. Calculations indicate that the nanocrystallites of γ–Al_2O_3 are packed fairly densely (i.e., the distance between the centers of the nanocrystallites is only slightly greater than the sum of their radii), a fact confirmed by the high-resolution studies of the nanocrystalline layer. This implies that the diffusion distances for Si (present in the matrix) is substantially larger than that for Al (present in the γ–Al_2O_3 nanocrystallites) required for complete composition homogenization. This causes an Al-rich core to remain within the γ–Al_2O_3 nanocrystallites, when the critical Al/Si ratio of 3 for mullite nucleation is reached in the region where interdiffusion between the matrix and the nanocrystallites has occurred.

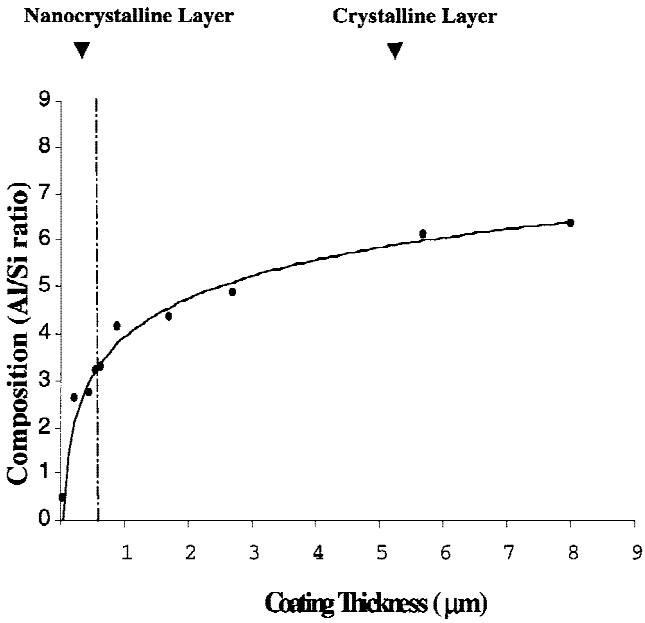

FIG. 7. Plot of Al/Si ratio across a CVD-mullite coating cross section.

It has been known from previous studies of mullite produced by sol-gel processes, that composition (Al/Si ratio), particle size and degree of mixing of precursor materials are important factors for mullite formation. In our CVD processing, the alumina and silica precursors are nanosized and mixed homogeneously. However, as mentioned before, a nanocrystalline coating alone formed cristobalite instead of mullite when annealed at 1200 °C. A chemical analysis of this layer by STEM, reveals that the maximum Al/Si ratio in this coating was less than the critical composition necessary for mullite nucleation. Thus, it appears that composition is the key factor that determines the nucleation of mullite grains. To verify this assumption, two nanocrystalline coatings were grown under the same deposition conditions as described above. However, a source for Al was provided in these coatings by growing a thin alumina-rich layer by CVD, at the coating surface and coating/substrate interface respectively, as shown in Fig. 8. Figure 8 shows that in both cases, mullite diffraction peaks were clearly seen after 100 h at 1200 °C, implying that the critical composition for mullite formation was reached by diffusion during the annealing. This validates our assumption that composition is the key factor for mullite nucleation in the nanocrystalline layer, and that mullite grains will nucleate when the Al/Si ratio reaches the critical value.

This requirement of the Al/Si ratio reaching a critical value for mullite nucleation also explains the trend of decreasing thickness of the nanocrystalline layer with increasing input $AlCl_3/SiCl_4$ ratios (Fig. 6). In all cases, due to the presence of native silica layer on the Si-based substrate, the initial coating is Si-rich. However, increasing the $AlCl_3/SiCl_4$ ratio increases the availability of Al atoms and allows for a short incubation time before the critical composition for mullite nucleation is reached, leading to the formation of the columnar mullite grains.

Diffusion plays a very important role in the mullite-formation process. In the sol-gel processing of mullite, the mullitization process via solid-state reaction depends on the bulk diffusion. The mullitization temperature is thus related to the degree of mixing of Al- and Si-containing species. A single-phase sol-gel in which aluminum- and silicon-containing precursors are mixed at a molecular scale will transform to mullite around 980 °C.[11] Precursors that are mixed at a micro scale or coarser require much higher temperatures, sometimes in excess of 1500 °C. One of the major advantages of growing mullite by the CVD process is that mullite can be

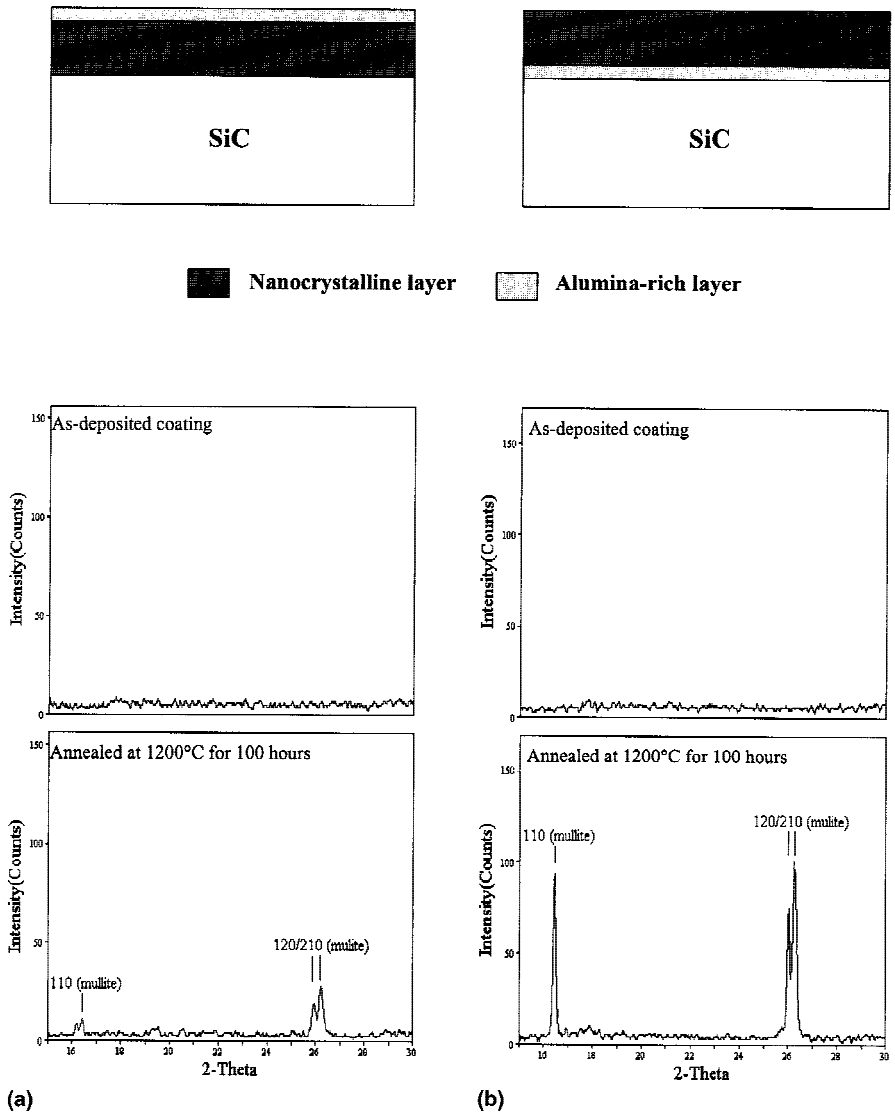

FIG. 8. Schematic of coating morphology and XRD patterns of the nanocrystalline coatings in the as-deposited state, and after a 100-h anneal at 1200 °C, when a thin alumina-rich layer was grown (a) at the top of nanocrystalline layer, and (b) at the nanocrystalline layer/substrate interface.

nucleated and grown at 950 °C, which is even lower than in the case of atomically mixed single-phase sol-gel processing. This is because coating growth in the CVD process relies on surface diffusion, which has much lower activation than the bulk-diffusion process required in coatings made by sol-gel processing. Additionally, growth rates in excess of 5 μm/h can be achieved by CVD, making it a very attractive process for the deposition of dense mullite coatings on complex geometries.

IV. CONCLUSIONS

Chemical vapor deposition (CVD) mullite coatings were deposited on SiC substrates by using the $AlCl_3$–$SiCl_4$–H_2–CO_2 system. A typical coating morphology consisted of two distinct layers. A layer adjacent to the substrate comprising of γ–Al_2O_3 nanocrystallites embedded in a vitreous SiO_2-based matrix, above which columnar mullite grains were present. The thickness of the nanocrystalline layer decreased as the input $AlCl_3/SiCl_4$ ratio was increased from 1 to 4. The Al/Si ratio in the coating increased monotonically from the coating/substrate interface to the coating surface in all cases. However, the composition at the boundary dividing the two regions was found to be similar for all samples examined in this study. When a critical Al/Si ratio of 3.2 ± 0.29 is reached, mullite crystals nucleate, and thereafter, the CVD process leads to the growth of columnar mullite grains directly.

ACKNOWLEDGMENTS

This research is sponsored by the United States Department of Energy, Contract No. DE-AC05-840R21400, and Martin Marietta Energy Systems, Inc., Contract No. SC-19X-SS110C.

REFERENCES

1. H. Schneider, K. Okada, and J.A. Pask, *Mullite and Mullite Ceramics* (John Wiley & Sons Ltd., Chichester, 1994).
2. R.P. Mulpuri and V.K. Sarin, J. Mater. Res. **11,** 1315 (1996).
3. V.K. Sarin and R. Mulpuri, U.S. Patent No. 5 763 008 (1998).
4. Powder Diffraction Files, International Center for Diffraction Data, Swathmore, PA, (1991).
5. Y. Nakajima, N. Morimoto, and E. Wanatabe, Proc. Japan. Acad. **51,** 173 (1975).
6. D. Doppalapudi and S.N. Basu, Mat. Sci. Eng. **A231,** 48 (1997).
7. W.E. Cameron, Am. Mineral. **62,** 747 (1977).
8. S. Komarneni and R. Roy, J. Am. Ceram. Soc. **68**(9), C-243 (1985).
9. S. Komarneni and R. Roy, J. Am. Ceram. Soc. **69**(3), C-42 (1985).
10. T. Yokoyama, K. Nishu, S. Torii, and Y. Ikeda, J. Mater. Res. **12,** 2111 (1997).
11. B.E. Yoldas in *Ceramic Transactions, Vol. 6, Mullite and Mullite Matrix Composites*, edited by S. Sōmiya, R.F. Davis, and J.A. Pask. (American Ceramic Society, Westerville, OH, 1990), p. 255.